High-speed characterization of submicrometer giant magnetoresistive devices

S. E. Russek,[a] J. O. Oti, and Shehzaad Kaka
Electromagnetic Technology Division, National Institute of Standards and Technology, Boulder, Colorado 80303

Eugene Y. Chen
Motorola, Semiconductor Technology-SPS, MD-EL308, 2100 East Elliot Road, Tempe, Arizona 85284

A microwave test structure has been designed to measure the high-speed response of giant magnetoresistive (GMR) devices. The test structure uses microwave transmission lines for both writing and sensing the devices. Pseudo-spin-valve devices, with line widths between 0.4 and 0.8 μm, were successfully switched with pulses whose full width at half-maximum was 0.5 ns. For small pulse widths τ_{pw} the switching fields are observed to increase linearly with $1/\tau_{pw}$. The increase in switching fields at short pulse widths is characterized by a slope which, for the current devices, varies between 4 and 16 μA s/m (50–200 Oe ns). The magnetoresistive response during rotation and switching was observed. For small rotations ($\sim$45° between layer magnetizations) the GMR response pulses had widths of 0.46 ns, which is at the bandwidth limit of our electronics. For larger rotations ($\sim$90°) the response pulses broadened considerably as the magnetic layers were rotated near the unstable equilibrium point perpendicular to the device axis. Full 180° switches of both soft and hard layers were observed with switching times of approximately 0.5 ns. © *1999 American Institute of Physics.* [S0021-8979(99)70308-7]

I. HIGH-SPEED GMR TEST STRUCTURE

In this paper we describe a microwave test structure which was developed to accurately measure the high-speed dynamics of GMR devices. Using this structure, we measured the high-speed switching behavior of pseudospin-valve devices with sub-micrometer line widths. We successfully switched the magnetic layers (180° reversal) with 0.5 ns write pulses and measured rotation and switching times. The rotation times can vary from 0.46 ns to several nanoseconds depending on the degree of rotation. The observed switching times are approximately 0.5 ns. We observed an increase in switching field, at short times, as the pulse width is decreased. The switching fields increase linearly with $1/\tau_{pw}$, where τ_{pw} is the full width of the pulse at half-maximum.

The high-speed test structures, shown in Fig. 1, were fabricated on both Al_2O_3 ceramic substrates and high resistivity Si substrates ($>2000\,\Omega$ cm). The structure uses three metalization layers, two dielectric layers, and one GMR layer. The sense lines are coplanar waveguides (CPW), fabricated in the base metal layer, which are exponentially tapered from a center-line width of 100 to 2 μm.[1] At the 2 μm end, the CPW line is jumpered to a microstrip sense line fabricated in the second metal layer. All of the transmission lines are designed to have 50 Ω impedances. The base metal layer serves as the ground plane for the microstrip lines. The microstrip sense line connects to the GMR device and is then shorted to the ground plane [Fig. 1(b)]. The sense line microstrip has a width of 1 μm and the active area of the GMR device is varied to obtain device resistances close to 50 Ω. The write line is formed from a CPW patterned in base metal layer and transitions to a 2 μm wide microstrip line patterned in top metal layer. The write line is a 2 mm long through-line and is terminated in 50 Ω off of the chip. The microstrip lines are long and fairly lossy. This keeps reflections from potential impedance mismatches away from the active device area; lossy lines insure that reflections are strongly damped. However, the lossy lines contribute to broadening of the observed pulses.

All of the measurements were carried out on a microwave probe station using coplanar probes with 18 GHz bandwidth. The write lines show approximately 7 dB attenuation at 10 GHz. The write and sense pulses were recorded on a 1.5 GHz bandwidth digitizing oscilloscope at 8×10^9 samples/s. The sense pulses were sent through a bias tee, which allows a dc to be injected into the device, and through a 25 dB, 1.3 GHz bandwidth amplifier before going to the digitizing oscilloscope. Typical incident and transmitted write pulses are shown in the inset in Fig. 1(a). There is a 13% reflection when the write signal goes on chip; the transmitted write pulse shows a voltage attenuation of 0.54.

The GMR devices used for this work were magnetic bilayers consisting of a thin (soft) magnetic layer, a thick (hard) magnetic layer, and a Cu spacer layer. The films were sputter-deposited using two different types of magnetic layer structures: (Ta 5.0 nm—$Ni_{0.8}Fe_{0.2}$9.0 nm—Co 1.0 nm—Cu 3.0 nm—Co 1.0 nm—$Ni_{0.8}Fe_{0.2}$4.0 nm—Ta 5.0 nm) and ($Ni_{0.65}Fe_{0.15}Co_{0.2}$6.0 nm—$Co_{0.95}Fe_{0.5}$ 1.0 nm—Cu 3.0 nm—$Co_{0.95}Fe_{0.5}$ 1.0 nm—$Ni_{0.65}Fe_{0.15}Co_{0.2}$ 2.0 nm—Ta 10.0 nm). The devices were patterned in nominally rectangular shapes, although the lithography and etching gives rounded ends. The magnetoresistance ratio for these devices varied from 6% to 8%. Low-frequency magnetoresistance versus write current and write field, for a 0.6 μm NiFe–Co device, is shown in Fig. 2. The write fields were taken as the magnetic field directly below the write line ($H=I/2w$, where w is the line width). The write line does not extend all across the GMR device, so parts of the device experience a field value

[a]Electronic mail: russek@boulder.nist.gov

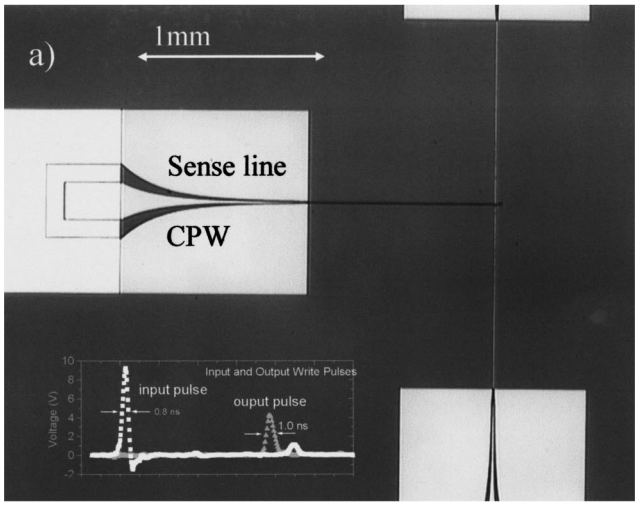

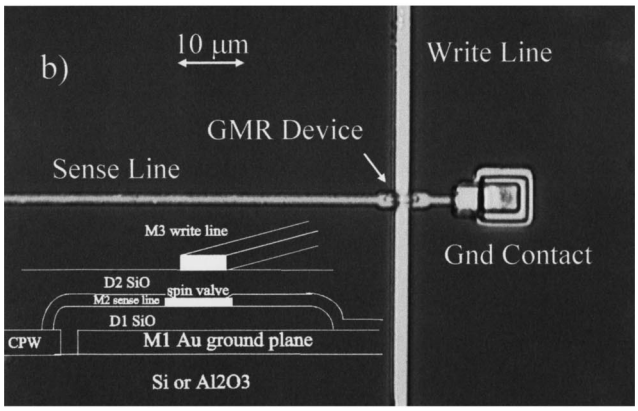

FIG. 1. (a) Micrograph of dynamical test structure showing sense and write waveguides. Inset shows an incident and transmitted write pulse. (b) Higher magnification of device area.

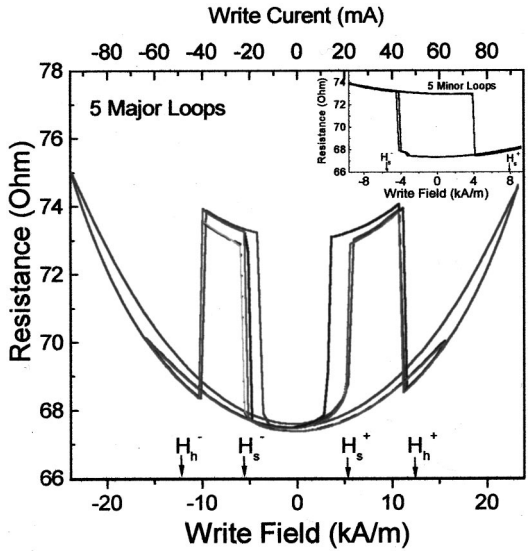

FIG. 2. Major loop magnetoresistance of a $0.6\times4.6\ \mu m^2$ NiFe–Co device as a function of write current and write field. Five traces are shown to illustrate degree of switching reproducibility. The inset shows the minor loops of the same device. The arrows in both figures indicate the hard and switching fields (H_h and H_s) for these devices determined by a uniform rotation simulation.

different from the nominal value. Figure 2(a) displays five minor loops (all from the same device) which show the switching of the soft layer and Fig. 2(b) displays five major loops showing switching of both the soft and hard layers. The curvature in the data is due to heating from the write line. The switching fields are considerably less than those predicted by coherent rotation models (shown by arrows in Fig. 2) and there is variation or jitter in the switching fields. This indicates that switching in these devices is more complicated than simple uniform rotation and that microdomains at the device ends and edges may be playing an important role in the reversal process.[2–4]

II. HIGH-SPEED SWITCHING

A series of write and sense pulses for a 0.6 μm wide NiFe–Co device are shown in Fig. 3. In the initial device state the soft and hard layers are oriented in the same direction, parallel to the long axis of the device. The sense current, which for these data was 1.0 mA, will cause the magnetizations of the soft and hard layers to rotate in opposite directions. The write pulse applies a field 180° with respect to the initial magnetizations. The measured transmitted write pulse width, as determined by a Gaussian fit, is 0.54 ns. The actual pulse width, taking into account the limited bandwidth of the digitizing scope, is 0.45 ns. Figure 3(a) shows a partial rotation, predominantly of the soft layer. The angle of rotation can be estimated by $\cos(\theta_R)=1-2V_{\text{peak}}/V_{180}$, where V_{peak} is the observed peak voltage and V_{180} is the measured change in voltage for a 180° switch. The rotation angle in Fig. 3(a) is approximately 45°. As the write pulse amplitude is increased, the sense pulse amplitude increases as the rotation angle increases. The pulse width also increases as the layers are rotated closer to the unstable equilibrium point with the magnetizations perpendicular to the device stripe. When the pulse height is increased further, irreversible switches occur as seen in Fig. 3(c). The event shown is not a full reversal of the soft layer since the voltage change is less than half that of a full switch. As the pulse height is increased further, both hard and soft layers completely switch (not shown in Fig. 3). At this point, further field pulses do not affect the magnetic state and no sense pulse is observed, as shown in Fig. 3(d). No sense signal is observed even for write pulses up to 15 V, indicating that these structures are highly decoupled except by the magnetic coupling through the devices.

Figure 4 shows complete soft and hard layer switching. The write pulses were systematically increased in 150 mV steps until switching occurred. Figure 4(a) shows the soft layer switching from a parallel to an antiparallel state. The switching event has a fast component from 0 to 1.5 mV, and a slower relaxation component from 1.5 to 2.2 mV. The duration of the fast part of the switching process can be quantified by the width of the derivative curve (Fig. 4) which yields a switching time of 0.49 ns. The slow component has a duration of $\sim$2 ns. The hard layer switching is shown in Fig. 4(b). In this case the resistance decreases, giving a negative pulse. This switching event also has a fast and a slow component with times similar to the soft layer switch.

The dependence of the switching fields on pulse width was measured for several devices and the data are shown for NiFe–Co device in Fig. 5. The pulse widths τ_{pw} were varied from 0.5 to 10 ns. The pulse shape for sub-nanosecond a 0.8

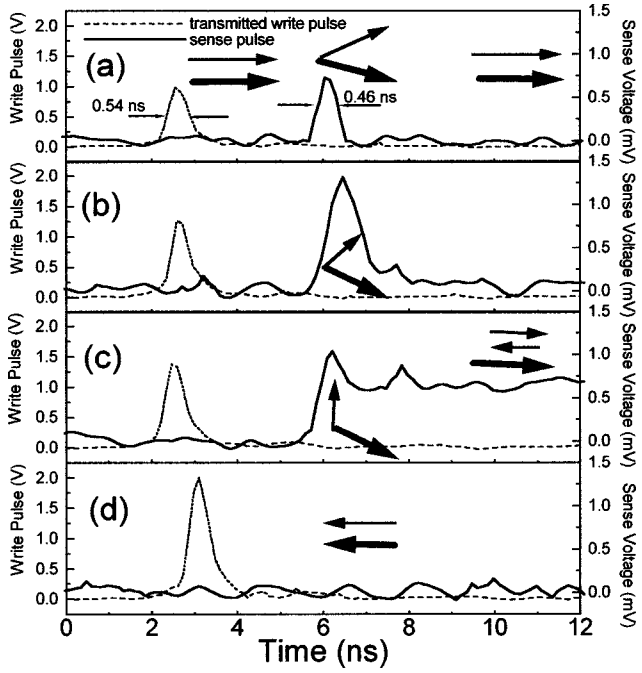

FIG. 3. Series of write and sense pulses for a $0.6\times4.6\ \mu m^2$ NiFe–Co device with 1 mA bias current: (a) partial rotation, (b) rotation near 90°, (c) partial irreversible switch of soft layer, and (d) after full switch of both layers. The thin and thick arrows schematically show the states of the soft and hard layers at particular times.

μm wide NiFeCo–FeCo device and 0.6 μm wide pulses are well fitted with Gaussian profiles, whereas the longer pulses were square pulses with a 0.5 ns rise time. As seen in Fig. 5, both the soft and hard switching fields increase approximately linearly with $1/\tau_{pw}$. The increase in switching fields can be characterized by the slope of the linear fits to the data. For the devices measured, the slope varied from 5.5 to 16 μA s/m (50–200 Oe ns).

III. DISCUSSION

The data presented here are qualitatively similar to what is observed in uniform rotation models. These simulations show a field-dependent latency period as the magnetizations move out of the low-torque regime, a fast switching as they are driven over an energy barrier, and a slower settling time

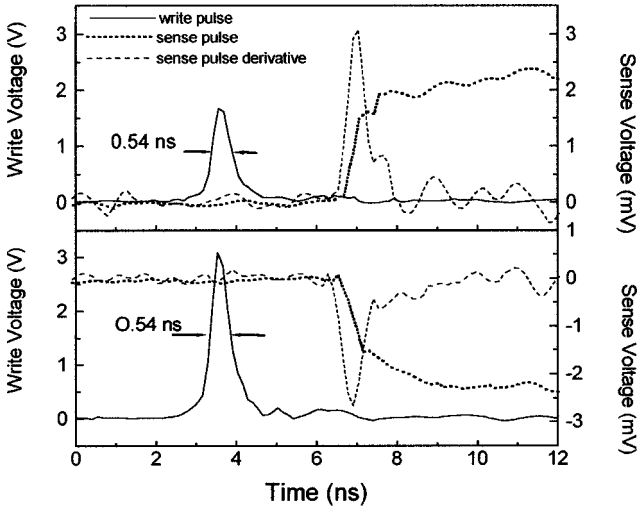

FIG. 4. (a) Switch of soft layer from parallel to antiparallel state in a 0.6 $\times$4.6 μm NiFe–Co device. (b) Subsequent switch of hard layer.

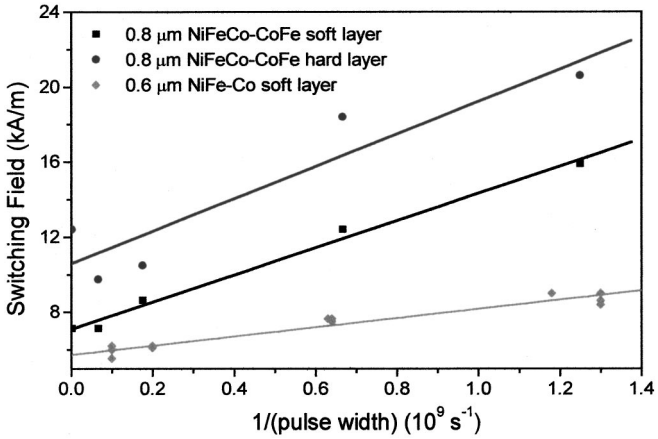

FIG. 5. Switching fields as a function of pulse width for a $0.8\times5.4\ \mu m^2$ NiFeCo–CoFe device and a $0.6\times4.6\ \mu m^2$ NiFe–Co device. The solid lines are fits to the data. Several measurements of the switching fields for the 0.6 μm device are displayed to illustrate the variation in switching field from run to run.

governed by the damping constant. The simulations indicate the switching time is fast, on the order of a few tenths of a nanosecond. This time is close to the present bandwidth of our electronics; our observed switching time is probably longer than the actual device switching time. The simulations show a complicated reversal and relaxation process since both layer magnetizations undergo large motions and are stongly coupled.[5] We do not see any free induction decay (motion with characteristic frequencies of the resonant modes of the system) as has been seen in large, single-layer Permalloy structures.[6,7] Many of the modes will be above our present bandwidth and we would have to average many switching processes to extract the signal. Switching in these devices will, in general, deviate considerably from uniform rotation;[3,4] however, many of the qualitative features such as a fast switching, slower relaxation, and free induction decay may be retained.

The linear dependence of switching field on inverse pulse width is consistent with many earlier switching studies of single-layer films which attributed the linear dependence to rotational dynamics.[8,9] Thermal activation processes, which have been observed in $1/f$ noise studies,[10] may also give rise to time dependent switching fields. Further work will be needed to determine the specific mechanism giving rise to the time dependent of the switching field in these devices.

[1] The design of the microwave transmission lines was done using standard methods such as those described in K. C. Gupta, *Microstriplines and Slotlines* (Artech House, Boston, 1996).
[2] Y. Zheng and J.-G. Zhu, IEEE Trans. Magn. **32**, 4237 (1996).
[3] J. O. Oti and S. E. Russek, IEEE Trans. Magn. **33**, 3298 (1997).
[4] J. Gadbois, J.-G. Zhu, W. Vavra, and A. Hurst, IEEE Trans. Magn. **34**, 1066 (1998).
[5] B. A. Everitt, A. V. Pohm, R. S. Beech, A. Fink, and J. M. Daughton, IEEE Trans. Magn. **34**, 1060 (1998).
[6] W. K. Hiebert, A. Stankiewicz, and M. R. Freeman, Phys. Rev. Lett. **79**, 1134 (1997).
[7] T. J. Silva, C. S. Lee, T. M. Crawford, and C. T. Rogers (unpublished).
[8] C. D. Olson and A. V. Pohm, J. Appl. Phys. **29**, 274 (1958).
[9] W. Dietrich, W. E. Proebster, and P. Wolf, IBM J. Res. Dev. **4**, 189 (1960).
[10] L. S. Kirschenbaum, C. T. Rogers, S. E. Russek, and Y. K. Kim, IEEE Trans. Magn. **33**, 3586 (1997).